

STUDY OF PION CAPTURE BY He<sup>3</sup>

## I. CHARGE EXCHANGE AND RADIATIVE CAPTURE

O. A. ZAIĀMIDOROGA, M. M. KULYUKIN, R. M. SULYAEV, I. V. FALOMKIN, A. I. FILIPPOV,  
V. M. TSUPKO-SITNIKOV, and Yu. A. SHCHERBAKOV

Joint Institute for Nuclear Research

Submitted to JETP editor December 30, 1964

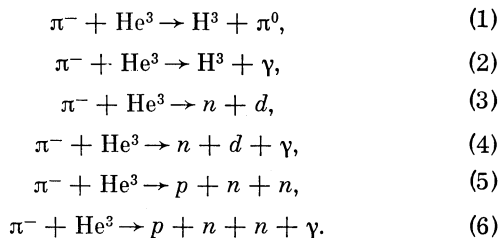
J. Exptl. Theoret. Phys. (U.S.S.R.) 48, 1267-1278 (May, 1965)

A high-pressure diffusion chamber operating in a magnetic field has been used to measure the ratio of the probabilities of charge exchange and radiative capture of pions by He<sup>3</sup> (the Panofsky ratio). The ratio was found to be  $2.28 \pm 0.18$ . On the basis of this ratio we have estimated the magnitude of the nuclear form factor, obtaining the value  $F^2 = 0.75 \pm 0.06$  for a momentum transfer  $q^2 = 0.47 F^{-2}$ . The relative probabilities of charge exchange and radiative capture are found to be  $W(H^3\pi^0) = (15.8 \pm 0.8)\%$ ,  $W(H^3\gamma) = (6.9 \pm 0.5)\%$ .

## 1. INTRODUCTION

INTEREST in the capture of stopped negative pions by He<sup>3</sup> nuclei results from the following circumstances. In the first place, the He<sup>3</sup> nucleus is one of the simplest nucleon systems and therefore can be used to trace the main features of pion absorption by nuclei. In the second place, the existence of the mirror nucleus H<sup>3</sup>, with a binding energy very close to that of He<sup>3</sup>, results in an unusual possibility of studying the charge exchange of pions in nuclei. Finally, in the capture of pions by He<sup>3</sup> we can expect an appreciable yield of the radiative capture process occurring without breakup of the nucleus.

According to the conservation laws the following processes can occur in the capture of  $\pi^-$  mesons by He<sup>3</sup>:



A theoretical discussion of  $\pi^-$ -meson capture by He<sup>3</sup> has been given by Messiah<sup>[1]</sup> and by Struminskiĭ.<sup>[2]</sup> Messiah obtained the ratio of the probabilities for the different channels, and the  $\gamma$ -ray spectrum. Struminskiĭ calculated the relative probabilities of the different processes, and the  $\gamma$ -ray and deuteron spectra in process (4), taking into account the final-state interaction. Both

of these authors assumed that pion capture occurs only from the S state of the  $\pi$ -mesic atom. This assumption affects only the estimate of the absolute capture probability. The ratio of probabilities of the different channels is practically independent of the channel from which the capture occurs, since the  $\pi$ -meson wave function does not enter into the probability ratio, and the difference in energies of the levels of the  $\pi$ -mesic atom is much less than the pion mass. The large uncertainty in the results of these calculations is due to well known difficulties of strong-interaction theory. Only in one case, the calculation of the so-called Panofsky ratio, i.e., the ratio between the probabilities of reactions (1) and (2), has it been possible to avoid these difficulties by inclusion of the experimental value of the Panofsky ratio for hydrogen.

The present paper, as well as our preliminary report,<sup>[3]</sup> is devoted to study of pion capture by He<sup>3</sup> with formation of tritium in the final state. The experimental value obtained for the Panofsky ratio for He<sup>3</sup>, together with the calculations of Struminskiĭ, is used to determine the nuclear form factor and the mean-square nuclear radius corresponding to the distribution of the centers of the nucleons.

The results of our study of other pion-capture processes in He<sup>3</sup> will be presented in a second paper.

## 2. EXPERIMENTAL APPARATUS

The study of pion capture by He<sup>3</sup> was performed with a high-pressure diffusion chamber in a magnetic field.<sup>[4]</sup>

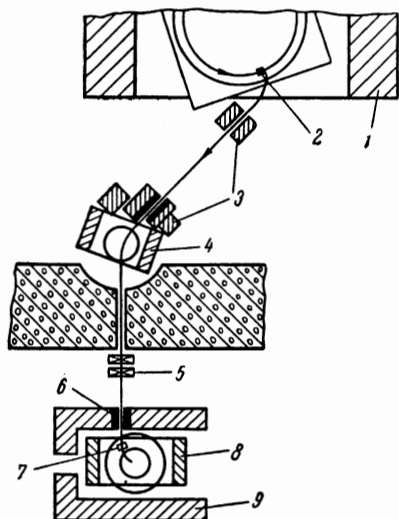


FIG. 1. Arrangement of the apparatus in the meson beam.

A diagram showing the arrangement of the apparatus in the pion beam is shown in Fig. 1.  $\pi^-$  mesons were produced in the JINR synchrocyclotron by bombarding a 5-mm-thick internal beryllium target 2 by 680-MeV protons. A 217-MeV/c  $\pi^-$  beam formed by the fringing field of the accelerator, before entering the diffusion chamber 8, passed through a bending magnet 4, a quadrupole lens 5, and a system of collimators 3 and 6. In front of the chamber, perpendicular to the beam trajectory, was placed a copper absorber 7, 45 mm thick. The value of the magnetic field in the chamber and the relative position of the chamber, the absorber, and collimator 6 were chosen so that the main part of the transmitted beam passed through the sensitive region of the chamber and the number of meson stoppings was maximized. The optimal value of the magnetic field turned out to be 6000 Oe. The absorber thickness was selected by measuring the differential range curve. The measurements were made with a telescope of three scintillation counters. The results of these measurements are shown in Fig. 2. A drawing of the range telescope is shown in the insert to the figure. The ordinate represents a quantity proportional to the number of particle stoppings in a 2-cm graphite block placed between counters  $C_2$  and  $C_3$ .

On slowing down the mesons in the chamber with a He<sup>3</sup> pressure of 17.5 atm, an average of one meson stopping per frame occurred. The contamination of  $\mu$ -meson stoppings amounted to 25% of the total number of stoppings.

The diffusion chamber operated under conditions of considerable ion loading produced by particles passing through the chamber and by back-

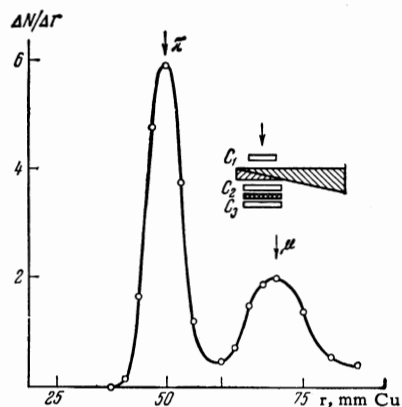


FIG. 2. Differential spectrum of meson stoppings.  $r$  – thickness of copper absorber between counters  $C_1$  and  $C_2$ ;  $dN/dr$  – number of meson stoppings in the graphite block between counters  $C_2$  and  $C_3$  for a given thickness of absorber.

ground in the region of the apparatus. The greatest complications were produced by slow neutrons which are captured by He<sup>3</sup> with a large cross section ( $\sim 5000$  b), forming a proton and triton ( $n + \text{He}^3 \rightarrow \text{H}^3 + p$ ). An effective protection from these neutrons was achieved by carefully surrounding the wiring duct into the experimental room by concrete blocks. In addition the apparatus was surrounded by local shielding of concrete, boron, and lead. These measures greatly reduced the background but it still remained appreciable. In each frame it was possible to observe tens of slow-neutron capture events. The presence of this background did not appreciably hinder the interpretation of meson-capture events in He<sup>3</sup>, but increased the recovery time of the chamber. The operating cycle of the chamber was 25 sec.

The processes of charge exchange (1) and radiative capture (2) are two-particle reactions with strictly determined secondary-particle energies. The energy of the tritium nuclei in these reactions is 0.19 and 3.28 MeV, respectively. Therefore the reactions can be distinguished by measurement of the triton ranges.

The radiative-capture events can be distinguished directly by measurement of the secondary-particle range spectrum, since the triton range from reaction (2) is 5.6 mg/cm<sup>2</sup> (22 mm at 17.5 atm).

Identification of charge-exchange events is complicated by the fact that the triton range from this reaction is small, amounting to 0.25 mg/cm<sup>2</sup> (1 mm at 17.5 atm). This small range hinders the identification of charge-exchange events as one-prong stars in the scanning. With an unfavorable orientation of the triton track with respect to the meson track, these events are difficult to distinguish from

Table I

Exposure number	H, Oe	P, atm	No. of photographs
I	12000	17.5	6400
II	6000	17.5	7650
III	12000	6.5	19100

zero-prong meson stoppings. On the other hand, the difficulty, which occurs for the same reason, in accurate measurement of range and spatial angles does not permit use of selection criteria which would control acceptance of these events in scanning. Therefore the selection of charge-exchange events according to secondary-particle range was supplemented by analysis of zero-prong stoppings according to the mass of the stopping meson. As a result it was possible to obtain the total number of pion stars in which the secondary-particle range was less than some easily measured value. These events will include all charge-exchange events. Then, to determine the number of charge-exchange events, we must subtract the background from other processes in a selected range interval.

Thus, in order to distinguish charge-exchange reactions, we must have a rather good resolution in the mass of the stopping meson. For this purpose we carried out an experiment with a considerably larger-than-optimum value of the magnetic field in the chamber. The yield of the radiative-capture reaction was expected to be almost three times smaller than the yield of the pion-charge-exchange reaction (taking into account the geometrical efficiency for detection). Therefore, in order to increase the accuracy in determination of the Panofsky ratio, we measured the yield of this reaction both in an experiment where the charge-exchange reaction was distinguished and in an experiment with the optimum magnetic-field value where reaction (1) was not distinguished. In addition it was desirable to perform an experiment at reduced  $\text{He}^3$  pressure, which allowed reaction (1) to be distinguished by direct measurement of the triton ranges. Data on the experimental conditions and the number of photographs obtained are given in Table I.

As a result, the Panofsky ratio for  $\text{He}^3$  was determined as the ratio of the probability of charge exchange, identified in Exposure I, to the probability of radiative capture, identified in Exposures I and II. The detection of pion charge exchange with reduced pressure in the chamber did not present difficulties, but the possibility of obtaining good statistics was severely limited by the low de-

tection efficiency for the radiative-capture events. The choice of the magnetic field in this exposure was not determined by the measurement of the Panofsky ratio but by the necessity of separating the secondary protons and deuterons produced in pion capture by  $\text{He}^3$ .

### 3. EXPERIMENTAL DATA AND ANALYSIS

The photographs obtained were double-scanned with the aid of a stereomagnifier. It was established that after the double scanning the efficiency for detection of meson stoppings in the chamber was close to 100%. Only those events were recorded in which the point of stopping of the meson was visible in both frames.

In the scanning we introduced the following classification of events:

1 ps — a one-prong star formed by a stopping meson, with the secondary-charged-particle range terminating in the sensitive region of the chamber;

1 pe — the same, but the secondary charged particle escapes from the sensitive layer of the chamber;

np — many-pronged star;

$\mu e$  —  $\mu$ -meson decay event, with visible decay electron;

stop — zero-prong meson stopping in the sensitive region;

stop\* — zero-prong meson stopping with unclear indications of a secondary-particle track;

$\mu e$ -star — meson-stopping event in which the secondary charged particle by visual estimation has an ionization close to minimum and the sign of the curvature is uncertain (the track is short or forms a small angle with the magnetic-field direction);

$\pi \mu e$  —  $\pi$ -meson decay event in which the  $\mu$  meson stops in the chamber and decays.

All of these events are easily identified by the characteristic change of track curvature of the stopping meson, and also by the curvature and ionization of the secondary-particle track. Identification is difficult for those events of group 1 ps when the secondary-particle track is near the boundary of the sensitive layer or in the region of the drop in sensitivity. In these cases the events were assigned to the class 1 pe. The zero-prong meson stoppings can be due to  $\mu e$  decay events in which the decay electron is not visible because of the closeness of the stopping to the insensitive region. Short-range pion-capture events in  $\text{He}^3$ , including charge-exchange events with unfavorable orientation of the secondary prong with respect to the meson track and pion stars with an invisible prong,

Table II

Exposure	Number of meson stoppings by groups								Number of $\pi\mu e$ -decay events		
	1 ps	1pe	$\mu e$	stop	stop*	$\mu e$ -star	np	unid <sup>1)</sup>	$\mu e$	stop	$\mu e$ -star
I	1102	2828	989	648	223	286	32	115	189	75	25
II	1329	3395	1233	593	309	376	43	157	104	40	22
III	427	1272	427	764	62	185	32	62	67	78	9

<sup>1)</sup>Unid = unidentified events.

also could be taken for zero-prong meson stoppings. Events occurring under complicated observation conditions (superposition of tracks, etc.) were assigned as unidentified events. To determine the total number of  $\pi$ -meson stoppings in Exposures I and II, we recorded  $\pi\mu e$  decays which were identified in accordance with the visibility of the decay electron, i.e., in the same way as  $\mu e$ -decay events.

$\pi^-$  mesons give only one-prong stars on capture in He<sup>3</sup>. Therefore the many-prong stars recorded must be assigned to the capture of pions by carbon and oxygen nuclei in the methyl alcohol vapor. The results of the scanning are given in Table II.

The range measurements were made in a projector which reproduced a picture of the event in space. In one-prong stars the following parameters were measured: 1) the track length of the stopping meson, 2) the coordinates of the stopping points of the meson and the secondary particle, 3) the length and width of the secondary-particle track, 4) the angle between the secondary-particle emission direction and the horizontal plane. In calculating the range we took into account the variation in gas density due to the temperature distribution in the sensitive region and made corrections for film shrinkage and finite track width.

#### 4. MEASUREMENT OF THE PANOFSKY RATIO IN He<sup>3</sup>

A. Experiments with a high pressure of He<sup>3</sup> in the chamber. Charge-exchange events were distinguished in Exposure I by determining, first of all, the total number of stars formed by stopping pions with a secondary-particle range  $< 0.5 \text{ mg/cm}^2$ . The choice of the range interval  $0-0.5 \text{ mg/cm}^2$  was based on two considerations. First, the range  $0.5 \text{ mg/cm}^2$  (2 mm at a pressure of 17.5 atm) is the minimum range which can be accurately measured. This could be verified in measurement of charge-exchange events in the experiment with reduced He<sup>3</sup> pressure, since the range of tritons from charge exchange in this case is 2.5 mm. Second, the efficiency for detection in the scanning of an event having such a secondary-particle range

was close to 100%.

Events with a range  $< 0.5 \text{ mg/cm}^2$  were extracted from the group of 1 ps stars by direct measurement of the range. To separate short-range pion stars from zero-prong stoppings (groups stop and stop\*) we made measurements of the meson masses. The meson masses were determined from the momentum and residual range. The measurements were made in a repro-jector with a variable-curvature template. In computing the momenta we took into account the non-uniformity of the magnetic field over the height of the sensitive layer. The following selection criteria were used in the mass measurements:

- 1) meson track length  $L \geq 50 \text{ mm}$ ,
- 2) the angle of inclination  $\alpha$  of the meson track, at the point of measurement of the radius of curvature, to the plane perpendicular to the magnetic-field direction did not exceed  $30^\circ$ .

To determine the resolution we made meson-mass measurements in the event groups  $\mu e$ , 1 ps, and 1 pe, i.e., for cases of reliable muon and pion stoppings selected in accordance with the criteria given above. These results are shown in Fig. 3. For the assumed separation boundary of  $125 \text{ MeV/c}^2$  the overlapping of the muon and pion mass histograms is small, amounting to about 10%. These results were used in separating pion events from

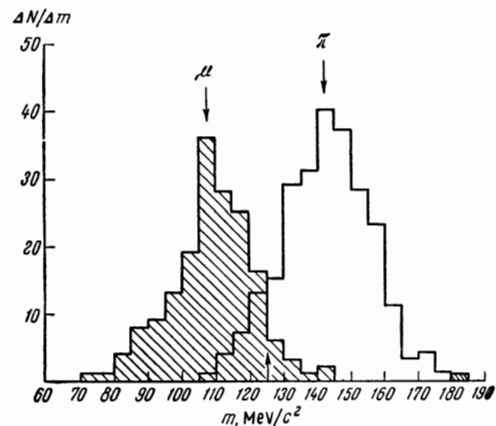


FIG. 3. Meson mass spectrum measured for positively identified cases of muon and pion stopping. The arrow indicates the assumed separation boundary.

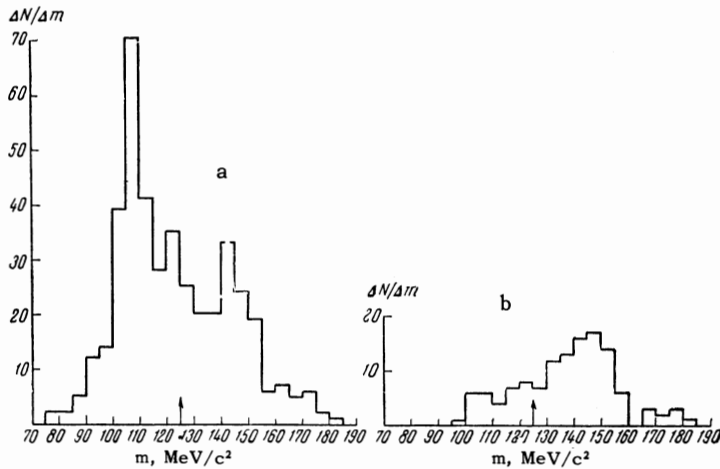


FIG. 4. Meson mass spectra, a – measured in the classification group stop; b – in the classification group stop\*.

zero-prong meson stoppings (groups stop and stop\*).

The measured spectra of the masses of particles producing zero-prong stoppings are shown in Fig. 4. It is evident from the figures that the events of group stop\* are mainly pion stoppings. A relatively large number of pion stoppings is included in the group stop. The total number of pion stoppings contained in zero-prong stoppings (groups stop and stop\*) was determined by taking into account the selection coefficient. On the basis of measurement of the distribution of stoppings in meson track length  $L$  and the angle  $\alpha$ , this coefficient was found to be  $0.61 \pm 0.03$ .

Finally, for separation of short-range pion stars from zero-prong stoppings, we considered the possibility that a zero-prong stopping can be due to a pion star with a fast secondary particle, whose prongs are not visible because of their proximity to the insensitive region. In this connection we determined a zone, bounded by the height of the sensi-

tive layer, in which practically all the electrons from  $\mu e$  decay were visible. The inefficiency of observation of a prong in a pion star in this zone was negligibly small, since the secondary particles from pion stars produce an ionization considerably larger than minimum. The number of zero-prong pion stoppings found in this zone was then extrapolated to the entire volume of the sensitive layer in accordance with the total number of meson stoppings.

The results of separation of pion stars with a secondary-particle range in the interval  $0-0.5 \text{ mg/cm}^2$  into the stopping classifications are as follows:

1ps	stop*	stop	total
$442 \pm 21$	$182 \pm 16$	$154 \pm 19$	$778 \pm 33$

The secondary-particle range spectrum from Exposure I is shown in Fig. 5a. It was obtained by measuring the lengths of prongs in the classifications 1 ps and 1 pe. From the 1 pe group only those

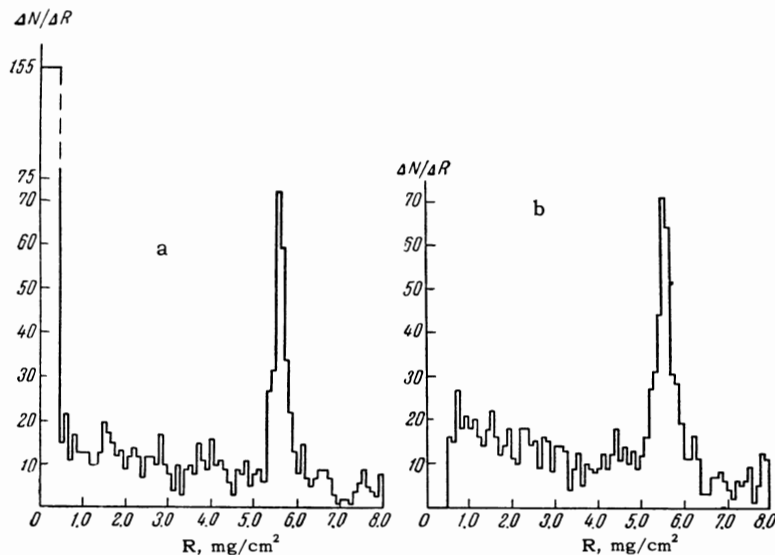


FIG. 5. Secondary-particle range spectra: a – from Exposure I in the range interval  $0-8 \text{ mg/cm}^2$ , b – from Exposure II in the interval  $0.5-8 \text{ mg/cm}^2$ .

Table III

Reaction	Exposure	Range interval, mg/cm <sup>2</sup>	Events recorded	Background	Detection efficiency	Final number of events
$\pi^- + \text{He}^3 \rightarrow \text{H}^3 + \pi^0$	I	0—0.5	778±33	61—4	1.0	717.2±33.0
$\pi^- + \text{He}^3 \rightarrow \text{H}^3 + \gamma$	I	4.8—6.3	320±18	104—9	0.71±0.02	304.5±29.2
	II	4.8—6.3	402±20	127—10	0.73±0.02	376.0±32.3

events were included in which the secondary-particle tracks had no  $\delta$  electrons and had an ionization of the order of that of a stopping meson. These events could be regarded as triton events from reactions (1) and (2). These selection characteristics for stars were introduced on the basis, which follows from an analysis of the 1 ps stars, that the track of a heavy stopping particle with a range < 14 mg/cm<sup>2</sup> does not have  $\delta$  electrons. Thanks to this criterion we have eliminated the possibility of admitting stars with terminating secondary-particle ranges, which could occur in identification of 1 ps events as the result of an indistinctly visible stopping of the secondary particle. Of course, this increases somewhat the background from nonmonochromatic particles. Furthermore, events in the range interval 0—0.5 mg/cm<sup>2</sup> are supplemented by events separated from the zero-prong stoppings.

In determination of the number of pion charge-exchange events it is necessary to subtract the background from other processes giving a contribution in the range interval 0—0.5 mg/cm<sup>2</sup>. The background value used is an average of that obtained by linear extrapolation of the background level from the neighboring range interval 0.5—1.5 mg/cm<sup>2</sup> and that obtained by extrapolation from this interval to zero. Since the background amounts to about 8%, the uncertainty in it does not have an important effect on the accuracy of the final result. The data relating to the separation of reaction (1) are listed in Table III below.

The separation of the radiative-capture reaction was made from the data of Exposures I and II. The measured secondary-particle range spectrum from Exposure II is shown in Fig. 5b. In this spectrum, as in the similar spectrum from Exposure I, along with the events of group 1 ps are included a part of the events from group 1 pe which satisfy the criteria given above. The average range of tritons from reaction (2) turned out to be 5.56 ± 0.01 mg/cm<sup>2</sup>. It agrees with the expected value of range for a 3.2-MeV triton. The detection efficiency for the mean range was calculated by the Monte Carlo method from experimental data on the distribution of meson stoppings in height and radius in the chamber. The background from other

reactions was determined from the adjacent regions to the right and left of the peak due to this reaction.

The results of the separation of the radiative-capture reaction in Exposures I and II are included in Table III.

The Panofsky ratio for He<sup>3</sup> on the basis of the experimental data of Exposures I and II can be found from the expression

$$P_{\text{He}^3} = N_{\pi^0} (N_{\text{I}} + N_{\text{II}}) / N_{\text{I}} (N_{\gamma\text{I}} + N_{\gamma\text{II}}), \quad (7)$$

where  $N_{\text{I}}$  and  $N_{\text{II}}$  are the total numbers of pion stoppings in Exposures I and II;  $N_{\gamma\text{I}}$  and  $N_{\gamma\text{II}}$  are the numbers of radiative-capture events found in the respective exposures, and  $N_{\pi^0}$  is the number of charge-exchange events in Exposure I.

To the total number of pion stoppings, besides the one-prong stars recorded, we must add those pion events which occurred among the zero-prong stoppings and in the  $\mu e$ -star classification. The results of identification of  $\pi\mu e$ -decay events were used for this purpose, since in this case the stopping  $\mu$  meson is reliably detected by means of the  $\pi\mu$  decay. Here we assumed an identical detection efficiency for the electron in  $\mu e$  and  $\pi\mu e$  decay events. In Exposure I the number of pion events in the zero-prong stoppings was obtained by two methods: directly on the basis of meson mass measurement, and by use of data on  $\pi\mu e$  decays. Data on the total number of pion stoppings are given in Table IV.

Using the data of Tables III and IV, we find from Eq. (7) that the Panofsky ratio in He<sup>3</sup> in the high-pressure experiments is

$$P_{\text{He}^3}^A = 2.27 \pm 0.19.$$

**B. Low-pressure experiment.** With a reduced He<sup>3</sup> pressure in the chamber (6.5 atm) the pion

Table IV

Exposure	Number of stoppings			Total number of stoppings
	stars	stop and stop*	$\mu e$ -star	
I	3930±63	446±29 <sup>1)</sup> 479±61	155±33	4531±75
II	4724±69	428±94	115±65	5267±133

<sup>1)</sup>On the basis of meson mass measurements.

Table V

Reaction	Range interval, mg/cm <sup>2</sup>	Events recorded	Background	Detection efficiency	Final number of events
$\pi^- + \text{He}^3 \rightarrow \text{H}^3 + \pi^0$	0.1–0.4	308 ± 17.6	46.2 ± 4.7	0.94 ± 0.02	278.2 ± 20.3
$\pi^- + \text{He}^3 \rightarrow \text{H}^3 + \gamma$	5.0–6.0	33 ± 5.7	4 ± 1.4	0.24 ± 0.02	119.8 ± 26.4

charge-exchange reaction can be distinguished directly by measurement of the triton range. The triton range from the charge-exchange reaction in this case is 2.5 mm, and from the radiative-capture reaction—56 mm. Figure 6a shows the measured secondary-particle range spectrum in the interval 0–1 mg/cm<sup>2</sup>. The mean range of tritons from reaction (1) turned out to be  $0.247 \pm 0.003$  mg/cm<sup>2</sup>. To the left of the peak corresponding to reaction (1), in the range interval 0–0.1 mg/cm<sup>2</sup>, the value of the background is unknown since the short-range events in this range interval are recorded with an efficiency less than 100% in the scanning. Therefore the background level, as in the high-pressure experiments, was determined as the average of the results of linear extrapolation from the neighboring interval on the right and from this interval to zero.

In Exposure III we recorded a small number of radiative-capture events, as the result of the low efficiency for detecting prongs of this length. The secondary-particle range spectrum for this exposure in the range interval 1–8 mg/cm<sup>2</sup> is shown in Fig. 6b. The detection efficiency for secondary-particle tracks of this length also was calculated by the Monte Carlo method on the basis of the measured distribution of meson stoppings in this exposure. The results of the separation of reactions (1) and (2) are shown in Table V. On the basis of these results the Panofsky ratio in He<sup>3</sup> is found to be

$$P_{\text{He}^3}^{\text{B}} = 2.32 \pm 0.54.$$

For a final value of the Panofsky ratio in He<sup>3</sup> we took the weighted mean of the two independent measurements A and B:

$$P_{\text{He}^3} = 2.28 \pm 0.18. \quad (8)$$

The relative probabilities of the charge-exchange and radiative-capture reactions were found to be the following:

$$W(\text{H}^3\pi^0) = (15.8 \pm 0.8) \%, \quad W(\text{H}^3\gamma) = (6.9 \pm 0.5) \%. \quad (9)$$

## 5. DISCUSSION OF RESULTS

In the work of B. V. Struminskiĭ<sup>[2]</sup> it was shown that the Panofsky ratio in He<sup>3</sup> can be expressed in terms of the Panofsky ratio in hydrogen and the ratio of the squares of the matrix elements (nuclear form factors) of the pion charge-exchange and radiative-capture processes. The Panofsky ratio in hydrogen is known with considerable accuracy at the present time and is equal to<sup>[5]</sup>

$$P_{\text{H}} = 1.533 \pm 0.024.$$

As a consequence of the small value of momentum transfer in the charge-exchange process, the matrix element for this process can be assumed to be unity. Therefore the Panofsky ratio in He<sup>3</sup> will depend only on the nuclear matrix element of the radiative-capture process. As a result the following relationship exists:

$$P_{\text{He}^3} = \frac{P_{\text{H}} \omega + M}{F^2} \frac{\omega_{\text{H}}}{\omega + m} \left[ \frac{EM}{E_{\text{H}}m} \left( \frac{\mu + m}{\mu + M} \right)^3 \right]^{1/2}, \quad (10)$$

where  $P_{\text{H}}$  is the Panofsky ratio in hydrogen,  $F$  is the nuclear matrix element for the radiative-capture process,  $\omega$  is the photon energy in reaction

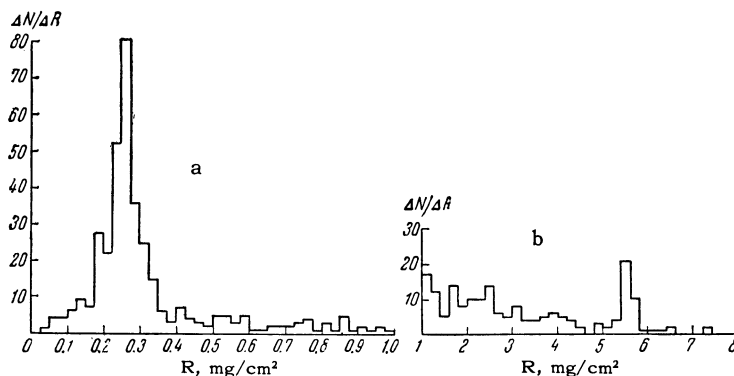


FIG. 6. Secondary-particle range spectrum from Exposure III: a — in the range interval 0–1 mg/cm<sup>2</sup>, b — in the range interval 1–8 mg/cm<sup>2</sup>.

(2),  $\omega_H$  is the photon energy in pion capture by hydrogen,  $m$  is the neutron mass,  $\mu$  is the  $\pi^0$ -meson mass,  $M$  is the triton mass,  $E$  is the energy released in process (1), and  $E_H$  is the energy released in  $\pi^-$ -meson charge exchange in hydrogen (the masses and energies of the particles are in MeV/c<sup>2</sup>).

The matrix element for the radiative-capture process is identical to the form factor  $F_1$  introduced by Schiff<sup>[6]</sup> for description of electron scattering by He<sup>3</sup> and H<sup>3</sup> nuclei. The experimental dependence of  $F_1$  on momentum transfer, obtained in the experiments of Hofstadter et al.<sup>[7]</sup> for the momentum-transfer region  $1-5 F^{-2}$ , is best described if the single-particle wave functions are chosen in the form of a Gaussian function or an Irving function with a mean-square radius

$$r = 1.5 \begin{matrix} +0.2 \\ -0.1 \end{matrix} F \quad \text{for a Gaussian function,}$$

$$r = 1.7 \pm 0.1 F \quad \text{for an Irving function.}$$

Using these results, we can calculate the value of the form factor  $F_1$  for a momentum transfer  $q^2 = 0.47 F^{-2}$  corresponding to the process of pion radiative capture. Taking into account the uncertainty in the choice of the single-particle wave function, we obtain

$$F_1^2(0.47) = 0.69 \pm 0.05.$$

After substitution of this value in (10) we obtain the expected value of the Panofsky ratio in He<sup>3</sup>:

$$P_{\text{He}^3}^{\text{theor}} = 2.47 \pm 0.16.$$

This value is to be compared with the experimental result:

$$P_{\text{He}^3}^{\text{exp}} = 2.28 \pm 0.18.$$

As we can see, the agreement is quite satisfactory, which indicates the validity of the methods used to calculate the ratio of the probabilities of the charge-exchange and radiative-capture processes for pions in He<sup>3</sup>.

The experimental value of the Panofsky ratio in He<sup>3</sup> can be used for an independent evaluation of the form factor  $F_1$  for a momentum transfer  $q^2 = 0.47 F^{-2}$ , i.e., for the momentum-transfer region which is practically inaccessible in electron-scattering experiments. Here it turns out that

$$F_1^2(0.47) = 0.75 \pm 0.06.$$

On the basis of this result we can obtain information on the mean-square radius of the nucleus. Because of the small value of momentum transfer in process (2), the different types of single-particle wave functions used by us (Gaussian, Irving, and exponential functions) give within a 2% spread the same values of mean-square radius, namely

$$r = 1.4 \pm 0.2 F.$$

The relative probabilities (9) obtained for the charge-exchange and radiative-capture reactions for pions in He<sup>3</sup> differ considerably from the theoretical estimates<sup>[2]</sup> of the yield of these reactions, which give the values  $W(\text{H}^3\pi^0) = 11.4\%$  and  $W(\text{H}^3\gamma) = 4.6\%$ . The large discrepancy of these values with the experimental result is first of all due to the fact that in the calculations of the relative probabilities of the charge-exchange and radiative-capture processes, in contrast to the calculation of the Panofsky ratio, use was made of perturbation theory, whose application in this case is poorly justified.

The authors are grateful to B. Pontecorvo and B. V. Struminskiĭ for discussion of their results and to A. G. Zhukov, N. V. Lebedev, V. I. Orekhov, V. F. Poenko, A. G. Potekhin, A. I. Tokarska, and E. A. Shvaneva for assistance in the measurements and carrying out the experiments.

<sup>1</sup> A. M. L. Messiah, Phys. Rev. **87**, 639 (1952).

<sup>2</sup> B. V. Struminskiĭ, JINR preprint E-1012; thesis; Proc. 1962 Intern. Conf. on High-Energy Physics, CERN, p. 17.

<sup>3</sup> Zaĭmidoroga, Kulyukin, Sulyaev, Falomkin, Filippov, Tsupko-Sitnikov, and Shcherbakov, JETP **44**, 1180 (1963), Soviet Phys. JETP **17**, 798 (1963).

<sup>4</sup> Aleksandrov, Zaĭmidoroga, Kulyukin, Peshkov, Sulyaev, Filippov, Tsupko-Sitnikov, and Shcherbakov, PTÉ **1**, 69 (1964), translation Instruments and Experimental Techniques, 1964 No. 1.

<sup>5</sup> Cocconi, Fazzini, Fidecaro, Legros, Lipman, and Merrison, Nuovo cimento **22**, 494 (1961).

<sup>6</sup> L. I. Schiff, Phys. Rev. **133**, B802 (1964).

<sup>7</sup> Collard, Hofstadter, Johansson, Parks, Ryneveld, Walker, Yearian, Day, and Wagner, Phys. Rev. Letters **11**, 132 (1963).